Analysis of the Energy Performance of Residential Inverter-Driven Heat Pumps

Francesco Benà[a*], Jacopo Vivian[a], Angelo Zarrella[a]

[a] Department of Industrial Engineering – Applied Physics Section, University of Padova, Via Venezia 1 – 35131, Padova, Italy

Abstract

The energy performance of heat pumps is usually declared by manufacturers in particular conditions. However, the energy consumption of heat pumps depends on real operating conditions and on key choices done at the design stage. In practice, the heat pump operates for large annual time at partial loads and in transient regime. These behaviours, together with the domestic hot water production (if provided) and the defrosting cycles (in air to water heat pumps), affect the energy performance of the machine.
In this paper, the real heat pumps performance is compared with a simplified modelling approach to evaluate the energy consumptions of the machines using data declared by manufacturers and with the reference Standard. To this purpose, the dataset reporting the operating conditions of ten installations made available by the open-source initiative HeatpumpMonitor is considered. Both air to water and ground source heat pumps are analysed. Two of these machines are compared in detail using the measured values, dividing the monitored data into stable conditions and transitory states. Then, the seasonal performance of the ten installations is compared with the corresponding value provided by manufacturers using the reference Standard. Finally, the simplified model is trained using the data declared by the manufacturers for four of the selected heat pumps in full and partial load operations. The model shows a relative mean error of 4% ranging between -8% and +14% in stable operations, and 6%, varying between -5% and 18% when all operative conditions are considered.

Keywords: Ground source heat pumps, Air source heat pumps, Heat pumps, Seasonal performance.

1. Introduction

Nearly 50% of the European Union's final energy demand is attributed to heating and cooling sector, with residential heating and cooling accounting for approximately 45% of this consumption [1]. One of the most promising technologies to replace old gas boilers, whose installation will be banned from 2040 [2] is the inverter-driven heat pump (IDHP) [3] thanks to its capability to modulate the speed of the compressor according to the thermal load request. This characteristic makes the design process of the heat pump (HP) particularly challenging because of the different temperature conditions that can be encountered during field operation.

During the design phase, engineers generally rely on technical standards. For example, in the EN 15450 [4], the HP is chosen on one single operative point, which is generally the coldest operative condition. Therefore, the HP can be oversized, since the unit does not usually operate in its design state. Several studies demonstrate the importance of proper design conditions for HP design and the potential deterioration of performance due to repeated transient operations if the chosen unit is oversized. For example, Dongellini et al. [5] found that the highest seasonal coefficient of performance (SCOP) occurs when the unit's design heating capacity (HC_{des}) is between 80% and 120% of the building's maximum heating demand. The coefficient of performance (COP)[6] can be penalised by the more frequent on-off cycle if the HC is too large compared to the heating

* Corresponding author. Tel.: +039-049-8276895
E-mail address: francesco.bena@phd.unipd.it

request. Xu et al.[7] showed that, for various configurations of air source heat pumps (ASHPs), start-up losses can account for between 2% and 17% of the total energy consumption in the analysed installation. Similarly, Madonna et al. [8] created a model based on field data to assess hourly performance, highlighting that the SCOP tends to decrease when the installed unit is oversized, as this leads to frequent on–off cycles.

A very promising renewable technology among all the possible IDHPs is the ground source heat pumps (GSHPs)[9]. The key advantage of this type of machine compared to the more traditional ASHPs is the use of the ground as a heat source-sink of the system. By means of a heat carrier fluid, in heating mode, the heat can be extracted from the ground and delivered to the evaporator [10]. Some studies demonstrate that, thanks to the almost constant temperature of the ground throughout the year, the performance of the GSHPs is generally higher compared to the ASHPs [11]. For example, Michopoulos et al. [12] experimentally demonstrated the energy consumption can be reduced by 45% if a GSHP is adopted compared to a traditional ASHP in the analysed installation. Sun et al. [13] simulated two GSHPs and two ASHPs, showing that the GSHPs maintain more than 80% of their efficiency when the external temperature drops. On the other hand, the ASHPs keep 55% of their original efficiency. Jonas et al.[14] simulated a GSHP and an ASHP coupled with solar thermal collectors, showing a generally higher seasonal performance in the first system compared to the second one in all the locations. Safa et al. [15] experimentally tested a ASHP and GSHP system in a twin house in Canada. Then, they extended the validity of the tests to other Canadian locations using TRNSYS, showing that the GSHP and the ASHP presented comparable performance results.

Despite the higher efficiency of this solution compared to ASHPs, the constraints on the design conditions remain important. For instance, Underwood [16] demonstrated using numerical simulations that a potential oversizing of the GSHP and of the heating system can decrease the efficiency up to 18%-22% for the two case studies analysed. Furthermore, the higher investment costs and payback time can be crucial in the choice of the correct unit during the design phase [17].

The necessity to identify a suitable methodology for the correct sizing of inverter-driven units and the proper selection of the type of HP remains an extremely important field of research. In this paper, a comparative analysis of the performance of ten different real installations, comprising five GSHPs and five ASHPs, is presented. To ensure variability in the study, the selected machines are from different series. First, to study the different temporal behaviour of the two kinds of machines, a time series analysis is performed on two installations with different sources during a cold day of the 2024-2025 heating season. Then, the SCOP defined by the Standard EN 14825 [18] ($SCOP_{st}$) is compared with the experimental one ($SCOP_{exp}$) for all installations to verify how much the standardised performance of the IDHPs differs from that of field operation, using two different analyses: the first considers only the stable operation of the units, while the second includes the transient regime as well. Finally, a simplified model approach is tested in one GSHP and three ASHPs.

2. Case studies

The field data of the ten different installations are available thanks to the HeatpumpMonitor [19] initiative, which provides an open-source database for monitoring the performance of in field HPs over a long period. All the installations are identified by acronyms (for example, *A05I01*), structured as follow:

- the first letter (in the example, A) indicates if the HP is an air source (A) or a ground source (G) unit;
- the first number identifies the nominal heating capacity (HC_{nom}) of the HP (in the example, 5 kW);
- The second letter and the last number (in the example, I01) indicate the number of the installation.

In Table 1, the main information of the system is reported, whereas in Table 2, all the main information about the building and the data availability for the analysed heating season are shown.

Each heat pump comes from a different series or a different manufacturer. The HPs are chosen among the ones present in the database according to the number of information reported in the corresponding catalogues for the evaluation of $SCOP_{st}$. Furthermore, each installation differs from the other in one or more of the features shown in Table 1. The installations are located in different parts of the United Kingdom, except for *G08I08*, which is in southern Germany, as displayed in Fig. 1.

Table 1. HVAC system main information. From left to right: installation ID, nominal heating capacity, source and refrigerant, design temperature, volume of the DHW (domestic hot water tank), temperature of the DHW and emission unit. In the last column, the possible emission units are New Radiators (NR), Old Radiators (OR), Fan Coil Radiator (FC) and Underfloor Heating (UFH).

ID	HC_{nom} [kW]	Source	Refrigerant	T_{des} [°C]	V_{tank} [L]	T_{dhw} [°C]	Emission Unit
G08I08	8	Ground	R410A	-10	0	-	Unknown
G08I06	8	Ground	R454B	-3	300	48	UFH
G11I10	11	Ground	R410A	-3	300	50	UFH
G12I03	12	Ground	R407C	-5	300	50	UFH + OR
G12I05	12	Ground	R454C	-3	300	50	UFH + OR
A05I07	5	Air	R290	-5	128	65	FC + OR + NR
A05I01	5	Air	R290	-3	250	48	NR
A10I09	10	Air	R32	-2	200	55	UFH
A10I04	10	Air	R32	-5	150	50	FC + OR
A13I02	13	Air	R32	-3	0	-	NR

Table 2. Building main information. From left to right: installation ID, Location, type of property, age, floor area. In the last column, the possible levels of insulation are no insulation (0), partial insulation (1), or full insulation (2).

ID	Location	Property	Age	Floor Area [m^2]	Insulation	Data availability
G08I08	Daisendorf, Germany	Semi-detached	1983 - 2011	240	2	01/09/24 - 30/04/25
G08I06	Ware, Hertfordshire	Detached	2012 or newer	244	2	01/09/24 - 30/04/25
G11I10	Ballyliffin, Co. Donegal, Ireland	Detached	2012	205	2	05/12/24 - 30/04/25
G12I03	Broxburn, West Lothian	Detached	1983 - 2011	185	2	01/09/24 - 30/04/25
G12I05	Shetland	Detached	2012 or newer	319	2	01/09/24 - 30/04/25
A05I07	Aberdeenshire	Semi-detached	1983 - 2011	76	2	25/09/24 - 30/04/25
A05I01	Sheffield	Semi-detached	1900-1939	98	1	23/12/24 - 30/04/25
A10I09	Okehampton, Devon	Detached	1900-1939	200	1	01/09/24 - 30/04/25
A10I04	Cadross, Dumbarton	Detached	Pre 1900	123	1	01/09/24 - 30/04/25
A13I02	Dinorwic, Gwynedd	Detached	1940-1982	168	1	01/09/24 - 30/04/25

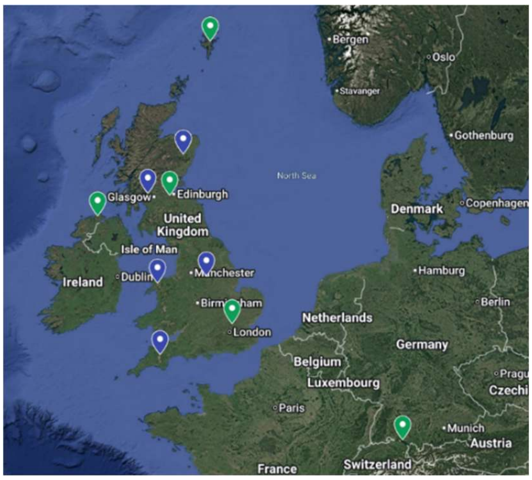

Figure 1. Map of the different installations. In green, GSHPs, in blue, ASHPs.

3. Methodology

In the first part of the Section, the method to identify the operative regimes of the machines is presented. In the second part, the process for calculating the seasonal energy efficiency according to (i) the Standard EN 14835 [18] ($SCOP_{st}$), (ii) using the monitored data ($SCOP_{exp}$) and (iii) using the simplified model ($SCOP_{mod}$) is briefly described. The supply and the return water temperature on the user's side are identified by the acronyms LExT (Load Exiting Temperature) and LET (Load Entering Temperature), whereas the entering temperature of the cold source is denoted by SET (Source Entering Temperature).

3.1. Status analysis

To identify the operating regime of the machine, a classifier method is proposed. To this end, at least one rated working condition in full-load operation must be obtained from the manufacturer's data. The thresholds are chosen according to the sensitivity analysis of the temporal series of the HPs. Eight functioning states are identified: *OFF, START, STOP, DHW, DEF, STEADY STATE, ACCELERATION* and *DECELERATION***.** In detail, the last states are identified as follows:

- *DHW status* corresponds to the condition in which the IDHP is heating up the tank for domestic hot water production. If the LExT rises above a defined threshold of 50 °C, it is supposed that the machine is producing domestic hot water.
- *DEF status* corresponds to the condition in which the ASHPs invert their operative refrigerant cycles to heat the evaporator for the defrosting cycle. It is assumed that ASHPs are defrosting if the temperature difference between LExT and LET drops below 0.5 K or if the heating capacity (HC) drops below 0 kW.
- *STEADY STATE, ACCELERATION and DECELERATION status.* The last two conditions are assigned when the machine is modulating to satisfy the building's heating demand. Instead, the *STEADY STATE status* refers to the operative condition in which the IDHP functions in a stable manner i.e. there are no rapid fluctuations in the observed variables. Thus, for the rest of the paper, the words steady state refer to the operative condition defined in Eq. (1).
  The three conditions are identified by the following Equation:

$$Status = \begin{cases} Steady\ State & if \ \left|\dfrac{HC_{t+1} - HC_{t-1}}{2\Delta\tau}\right| \leq c_{thrs}\, HC_{des} \\ Acceleration & if \ \dfrac{HC_{t+1} - HC_{t-1}}{2\Delta\tau} > c_{thrs}\, HC_{des} \\ Deceleration & if \ \dfrac{HC_{t+1} - HC_{t-1}}{2\Delta\tau} < -c_{thrs}\, HC_{des} \end{cases} \quad (1)$$

  where $\Delta\tau$ is the 5-minutes time step considered for the analysis (the variables correspond to their mean values evaluated over a 5-minute time interval) and c_{thrs} is equals to 0.05 for the ASHPs. A threshold coefficient c_{thrs} of 0.1 prevents the classifier from identifying the modulation regimes in units with lower HC_{nom} since it fails to highlight conditions of rapid deceleration or acceleration. On the other hand, a broader boundary (e.g. c_{thrs} equal to 0.01) classifies some working points as transitory states, even though they represent slow accelerations/decelerations (10 – 15 min) with respect to an operative cycle of the ASHPs, and therefore comparable to a stable functioning regime. Because the GSHPs operate more stably compared to the ASHPs, a strict gap is required to identify the transient regimes. Thus, for this type of machine, the coefficient c_{thrs} is chosen equal to 0.01.

According to the adopted status identification, some operative points could be classified as *DEF* because the temperature drops below 0.5 K despite being different operational states. However, since the maximum number of identified *DEF* states is around 3.5% among all the installations, the effects of possible misclassification of these events is contained when only steady state operation points are considered (the maximum error equals to 1.75% in the model and to 3.33% in the experimental calculation). Furthermore, the event misclassification does not affect the results if all operative conditions are considered.

The installations *A10I04* and the installation *G12I03* are analysed in detail. The distance between the two installations is approximately 70 km, thus no great differences between the external temperatures are expected. Furthermore, the two heat pumps have comparable HC_{nom} of 10 and 12 kW. However, the two installations differ significantly from one another. First, the monthly average values of the outdoor temperature T_{ext}, LET, LExT, absorbed power P, heating capacity HC and coefficient of performance COP are evaluated. Then, the classifier is applied to study the dynamics of the two systems on a cold day (10/01/2025) during the heating season.

3.2. $SCOP_{st}$ calculation

Standard EN 14825 [18] provides a comprehensive method description for calculating the SCOP. The Standard defines the $SCOP_{st}$ as:

$$SCOP_{st} = \frac{Q}{E} \tag{2}$$

where Q is the reference annual heating demand and E is the corresponding annual electricity demand. For the calculation of the two energy values, the Standard EN 14825 requires the assumption of a specific climate in which the machine is expected to be installed. Three choices are possible:

- *Cold climate conditions:* temperature conditions characteristics of Helsinki;
- *Warm climate conditions:* temperature conditions characteristics of Athens;
- *Average climate conditions:* temperature conditions characteristics of Strasburg.

For each weather condition, a different number of operating hours corresponds to the temperature bins, which are intervals of external air temperature ranging from -30 °C to 15°C, with an increment of 1°C. Except for *G08I08*, all the other installations are in the United Kingdom. Looking at the Köppen- Geiger classification [20], the UK weather is classified as temperate. Thus, the *average climate condition* is chosen for the analysis.

Once the weather conditions are selected, it is necessary to define the design LExT at which the unit is expected to operate. Since all the installations in the case studies present a discrete level of insulation, the chosen design LExT temperature for the study is 35°C. The values of $SCOP_{st}$ evaluated by manufacturers for these specific conditions are obtained from their catalogues.

3.3. $SCOP_{exp}$ calculation

The experimental SCOP ($SCOP_{exp}$) is evaluated through the measured values of heating capacity (HC_{exp}) and electrical absorbed power (P_{exp}):

$$SCOP_{exp} = \frac{\sum_{i=1}^{n} HC_{exp,i} \Delta\tau_i}{\sum_{i=1}^{n} P_{exp,i} \Delta\tau_i} \tag{3}$$

To calculate the influence of the transient regimes, the SCOP is obtained by considering solely the steady state conditions ($SCOP_{exp,ss}$) and all operative conditions ($SCOP_{exp,all}$). The relative error of the Standard EN 14825 [18] is calculated both for the steady state and for all the operative conditions:

$$RE_{st} = \frac{SCOP_{st} - SCOP_{exp}}{SCOP_{exp}} \cdot 100 \tag{4}$$

3.4. $SCOP_{mod}$ calculation

The model developed for the calculation of performance of the heat pumps in real installation is based on two variables, which are the part load ratio (PLR) and the power ratio (PR), calculated as:

$$PLR = \frac{HC_{pl}(SET, LExT)}{HC_{fl}(SET, LExT)} \tag{5}$$

$$PR = \frac{P_{pl}(SET, LExT)}{P_{fl}(SET, LExT)} = \alpha PLR + \beta PLR \cdot \frac{\Delta T - \Delta T_{min}}{\Delta T_{max} - \Delta T_{min}} + \varepsilon \tag{6}$$

where HC_{pl} and P_{pl} are the heating capacity and the electrical power in partial load operation at the given SET and LExT, whereas HC_{fl} and P_{fl} are the heating capacity and the electrical power in full load operation at the same temperatures. The model calculates PR as a function of PLR and of the temperature difference between LExT and SET (ΔT). The coefficients α and β are obtained using the ordinary least squares method on the catalogue point of the machines. The $SCOP_{mod}$ is obtained for both steady state and all the operating conditions as follows:

$$SCOP_{mod} = \frac{\sum_{i=1}^{n} HC_{exp,i}\Delta\tau_i}{\sum_{i=1}^{n} PR_i \cdot P_{fl,i}\,\Delta\tau_i} \tag{7}$$

To have a valuable result from the equations, the model requires a minimum of 3 catalogue points in partial load and the corresponding operative conditions in full load. Because of the scarcity of manufactures' data in partial load operation, solely four installations are suitable to be used for the calculation: one GSHP (*G11I10)* and three ASHPs (*A05I01, A10I04* and *A10I09*). The relative error of the model is calculated using Eq. (8) for both simulations:

$$RE_{mod} = \frac{SCOP_{mod} - SCOP_{exp}}{SCOP_{exp}} \cdot 100 \tag{8}$$

4. Results

In the first part, a comparison is presented between the performance of installations *A10I04* and *G12I03*.Then, the differences between $SCOP_{exp}$ and $SCOP_{st}$ are described. Finally, the model's results are compared with the experimental ones.

4.1. Monthly average performance

The monthly average values of T_{ext}, LET, LExT, P, HC and COP are reported in Table 3 for *A10I04* and *G12I03.* On average, the COP of the GSHP is higher than that of the ASHP, with the only difference being the one evaluated in April. This is probably due to the higher LExT for the ground source unit in this month. Generally, the ASHP operated at a greater LExT compared to the GSHP. This could be related to the lower level of insulation, the final user settings, or the installed emission units.

Table 3. Monthly average performance of *A10I04* and *G12I03*

	A10I04						G12I03					
Month/Year	SET [°C]	LET [°C]	LExT [°C]	HC [kW]	P [kW]	COP [-]	SET [°C]	LET [°C]	LExT [°C]	HC [kW]	P [kW]	COP [-]
09/2024	12.4	26.8	28.6	1.14	0.24	4.75	11.8	24.5	27.2	1.62	0.28	5.70
10/2024	11.0	29.4	31.5	1.85	0.38	4.89	10.5	26.5	29.0	2.29	0.45	5.10
11/2024	7.1	32.7	36.6	3.46	0.94	3.68	6.4	29.1	33.0	3.56	0.75	4.77
12/2024	7.1	33.0	37.2	3.67	0.98	3.75	7.0	28.6	32.8	3.78	0.79	4.81
01/2025	4.2	34.6	39.3	4.17	1.24	3.37	3.2	30.4	35.7	4.75	1.09	4.37
02/2025	5.4	33.1	37.5	3.90	1.01	3.87	5.2	29.8	34.5	4.18	0.92	4.54
03/2025	7.7	31.4	34.9	3.05	0.71	4.32	7.2	30.2	34.1	3.42	0.75	4.57
04/2025	9.9	28.3	30.7	2.06	0.44	4.74	9.2	29.7	32.5	2.65	0.59	4.47

4.2. Time series analysis

In Figs. 2(a) and 2(b), the temporal series of a cold day during the heating season for installation *A10I04* and installation *G12I03* are shown. Due to the low SET, the ASHP must defrost frequently. The total number of defrosts is 27, and the average distance between two of them is approximately 50 minutes. The repetitive acceleration and deceleration often lead the ASHP to operate in a transient state, as the continuous inversion of the cycle for defrosting decreases the LExT, compromising its stability.

On the other hand, the pattern of the GSHP is completely different: LExT is much more stable compared to the ASHP thanks to the complete absence of defrost. Some transitory states are still present in the functioning of the unit, such as the DHW generation at 15:45 and the modulation to follow the building's load between 18:00 and 20:00. The lower energy consumption in the colder months is due both to the lower LExT compared to the ASHP and to the more stable operating conditions. In fact, even if the LExT set point of the ASHP was lower, the system would not have the time to stabilise in that condition due to the defrost safety routine. This is clearly visible in Fig. 2(a), where, between 15:00 and 18:00, after an initial peak of P and LExT, the supply temperature tends to decrease, without reaching stability due to the subsequent defrost state. Overall, the continuous peaks of P and LExT penalise the performance of the machine.

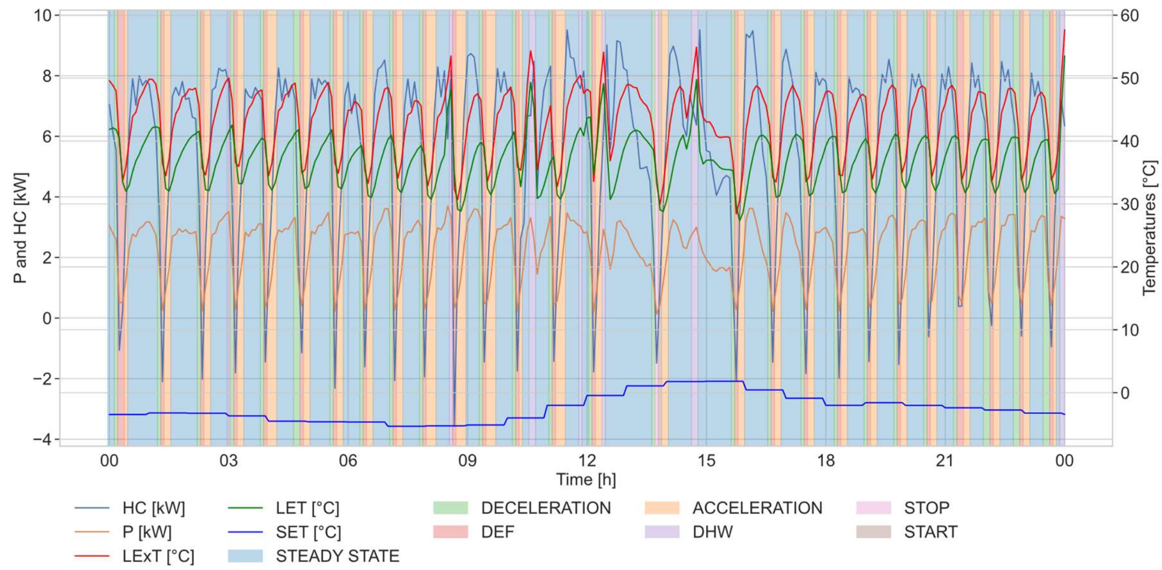

(a)

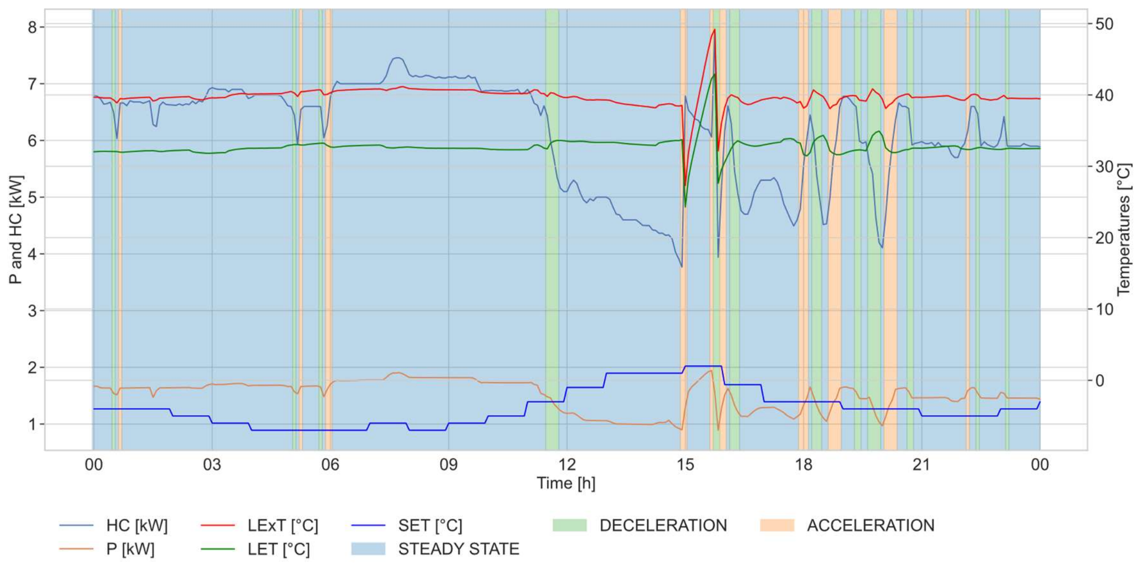

(b)

Figure 2. Time series analysis in installation *A10I04* (a) and *G12I03* (b) during 10/01/2025.

4.3. Comparison between standardised and experimental SCOP

In Fig. 3, the comparison between $SCOP_{st}$, $SCOP_{exp,ss}$ and $SCOP_{exp,all}$ is shown. In both cases, the value of the Standard EN 14825 [18] overestimates the experimental measurements. In particular, the mean RE_{st} for the GSHPs is equal to 22% in the range 9%-47% in steady state, whereas in all operative conditions it varies between 8% and 47%. On the other hand, the mean RE_{st} for the ASHPs in steady states is equal to 19% in the range 6%-34%, whereas, in all operative conditions, it increases to 25%, varying between 10% and 39%. Indeed, the difference between the two values of SCOP is more significant in the case of ASHPs compared to GSHPs. This is because the number of transient conditions (mainly due to defrosting on colder days) is significantly larger in the case of ASHPs.

In all installations, the $SCOP_{st}$ overestimates the real heat pumps' performance both in steady state and considering all the operating conditions. The reason can be related to the conservative approach used for the calculation of SCOP: the Standard EN 14825 suggests using LExT at one of 35, 45 or 55°C or variable LExT depending on the application. However, most manufacturers give SCOP at a constant supply temperature. In real applications, the machines operate at very different temperature ranges depending on the external conditions and on the set point. As a result, the actual performance of the IDHPs can differ drastically from the standardised one.

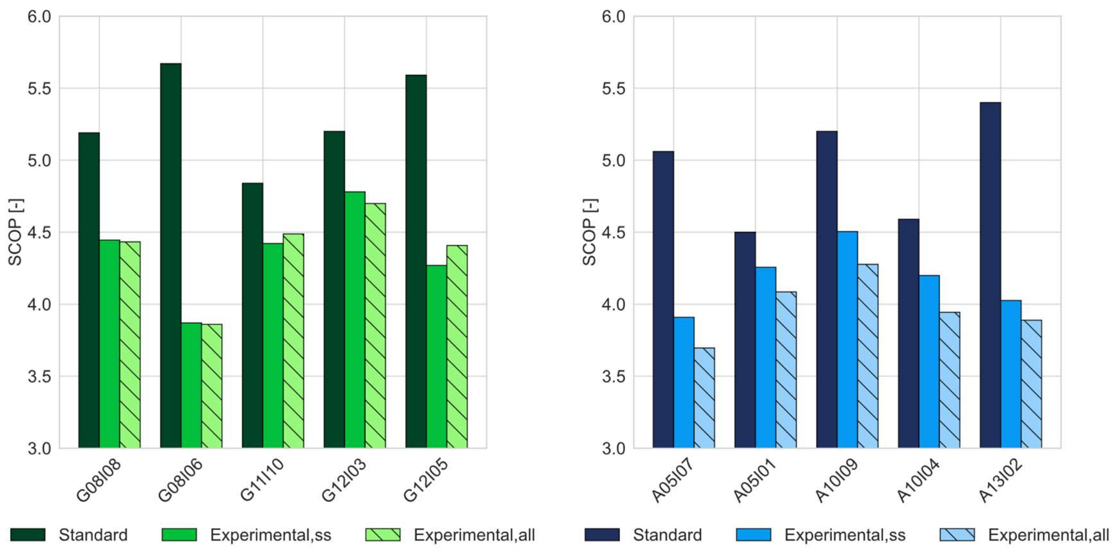

(a) (b)

Figure 3. SCOP experimental compared with SCOP calculated from normative EN 14285 with GSHPs (a) and ASHPs (b).

Overall, despite the $SCOP_{st}$ can be used as a first approximation of the performance of the unit to compare similar machines during the design phase of the system, it should not be the only metric to use as an evaluation source. Other factors, such as the in-field operation with similar installations, should be considered during the design phase.

4.4. Comparison between experimental and modelled SCOP

In Fig. 4, $SCOP_{mod}$ is compared with the $SCOP_{exp}$ for both the steady state and all the operative conditions. The results obtained from the model are comparable in both figures, indicating that the influence of the transitory regimes in the model prediction is contained. In fact, the mean relative error between the experimental and the modelled SCOP is almost 4% in steady state and around 6% when all conditions are considered. The model presents the larger error in installations *G11I10* (14% in steady state, 13% in all operative conditions) and *A10I09* (13% in steady state, 18% in all operative conditions), whereas in installation *A10I04*, the smallest RE_{mod} is obtained (-3% in steady state, -0.5% in all operative conditions). It should be noticed that the model can both overestimate and underestimate the SCOP depending on the training points used for the calculations. Further verifications on other installations are required to check the accuracy of the model.

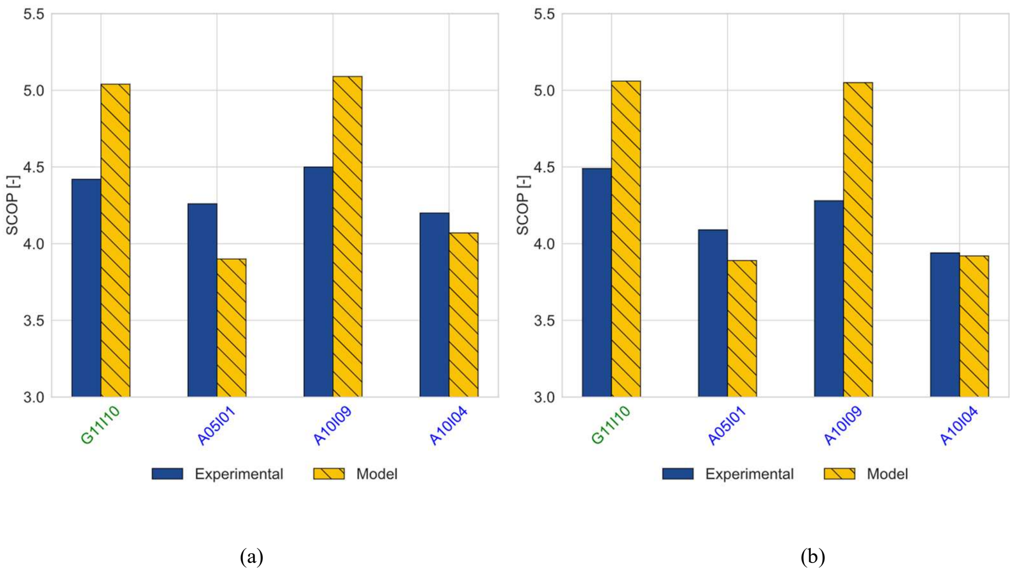

Figure 4. $SCOP_{mod}$ compared with $SCOP_{exp}$ both for the steady state (a) and for all the operative conditions (b).

5. Conclusions

In this paper, a performance analysis of a ground and an air source heat pumps is presented. Then, the real performance of ten different heat pumps is compared with the seasonal efficiency proposed by Standard EN 14825.The installations are chosen among different heat pump series to assure variability of the sample and with the catalogue's data necessary to perform the analysis. Finally, the differences between the experimental and modelled SCOP are commented. The analysis shows that:

- the average COP of the ground source heat pump is generally higher than that of the air source unit, thanks to the more favourable temperature of the thermal source, the influence of the system installations and of the user settings.
- during the cold day, the COP of the air source heat pump is heavily penalised by the continuous defrost states necessary to guarantee a safe operation of the unit. On the other hand, the performance of the ground source heat pump is much more stable, ensuring at almost constant load supply temperature.
- in the comparison between Standard EN 14825 and the real performance, the average relative error between the experimental and standardised SCOP for air and ground source heat pumps is respectively equal to 19% and 22% in steady state operation, whereas it is equal to 25% and 2% in all operative conditions, indicating a larger influence of the transitory states on the performance of the air source units. These differences are related to how the machines operate, continuously changing the supply temperatures to adapt to the load request.
- the mean relative error between the experimental and the modelled SCOP is almost 4% in steady state and around 6% when all conditions are considered. The effects of the transient states on the model performance appear to be contained. The results are based on just four installations and a further analysis is required to extend model reliability.

Future work will be related to the study of the oversizing of the units in the field applications, knowing the actual heating demand of the buildings. Furthermore, other research of the model reliability is necessary, extending if possible the sample size in analysis with other heat pumps.

Nomenclature

COP	Coefficient of performance	[-]
E	Annual electricity demand	[kWh]
HC	Heating capacity	[W]
LET	Load entering temperature	[K]
LExT	Load exiting temperature	[K]
P	Power	[W]
Q	Reference heating demand	[kWh]
PLR	Partial load ratio	[-]
PR	Power ratio	[-]
RE	Relative error	[%]
SCOP	Seasonal coefficient of performance	[-]
SET	Source entering temperature	[K]
T	Temperature	[K]
ΔT	Temperature difference	[K]
V	Volume	[L]
Δτ	Temporal interval between two measurements	[s]

Subscripts

des	Design
dhw	Domestic hot water
exp	Experimental
ext	External
fl	Full load
max	Maximum
min	Minimum
mod	Model
nom	Nominal condition
pl	Partial load
st	Standard
thrs	Threshold

Acknowledgements

The authors gratefully acknowledge the people behind the OpenEnergyMonitor project for making the heat pump data openly available through the HeatpumpMonitor initiative.

References

[1] Kavvadias K, Jiménez-Navarro JP. Decarbonising the EU heating sector Integration of the power and heating sector, n.d. https://doi.org/10.2760/943257.
[2] Office of the European Union L- P, Luxembourg L. DIRECTIVE (EU) 2024/1275 OF THE EUROPEAN PARLIAMENT AND OF THE COUNCIL of 24 April 2024 on the energy performance of buildings. 2024.

[3] Qureshi TQ, Tassou SA. VARIABLE-SPEED CAPACITY CONTROL IN REFRIGERATION SYSTEMS. vol. 16. 1996.
[4] European Committee for Standardization-CEN. EN 15450:2007, Heating systems in buildings-Design of heat pump heating systems 2007.
[5] Dongellini M, Naldi C, Morini GL. Sizing effects on the energy performance of reversible air-source heat pumps for office buildings. Appl Therm Eng 2017;114:1073–81. https://doi.org/10.1016/j.applthermaleng.2016.12.010.
[6] Prud'homme S, Breton S, Tamasauskas J, Sager J. A Simulation-Based Exploration of Air-Source Heat Pump Sizing in Canada. 11th Conference of IBPSA n.d.
[7] Xu Z, Li H, Xu W, Shao S, Wang Z, Gou X, et al. Investigation on the efficiency degradation characterization of low ambient temperature air source heat pump under partial load operation. International Journal of Refrigeration 2022;133:99–110. https://doi.org/10.1016/j.ijrefrig.2021.10.002.
[8] Madonna F, Bazzocchi F. Annual performances of reversible air-to-water heat pumps in small residential buildings. Energy Build 2013;65:299–309. https://doi.org/10.1016/j.enbuild.2013.06.016.
[9] Lim H, Kim C, Cho Y, Kim M. Energy saving potentials from the application of heat pipes on geothermal heat pump system. Appl Therm Eng 2017;126:1191–8. https://doi.org/10.1016/j.applthermaleng.2017.04.086.
[10] Bayer P, de Paly M, Beck M. Strategic optimization of borehole heat exchanger field for seasonal geothermal heating and cooling. Appl Energy 2014;136:445–53. https://doi.org/10.1016/j.apenergy.2014.09.029.
[11] Wang G, Wang W, Luo J, Zhang Y. Assessment of three types of shallow geothermal resources and ground-source heat-pump applications in provincial capitals in the Yangtze River Basin, China. Renewable and Sustainable Energy Reviews 2019;111:392–421. https://doi.org/10.1016/j.rser.2019.05.029.
[12] Michopoulos A, Bozis D, Kikidis P, Papakostas K, Kyriakis NA. Three-years operation experience of a ground source heat pump system in Northern Greece. Energy Build 2007;39:328–34. https://doi.org/10.1016/j.enbuild.2006.08.002.
[13] Sun J, Li Y, Kashif N, Liu X, Lian J, Pagnotti A, et al. Comparative performance assessment of air-source and ground-source heat pumps using CO_2 and R-410A with water well integration: A simulation study. Journal of Building Engineering 2025;114. https://doi.org/10.1016/j.jobe.2025.114453.
[14] Jonas D, Frey G, Theis D. Simulation and performance analysis of combined parallel solar thermal and ground or air source heat pump systems. Solar Energy 2017;150:500–11. https://doi.org/10.1016/j.solener.2017.04.070.
[15] Safa AA, Fung AS, Kumar R. Comparative thermal performances of a ground source heat pump and a variable capacity air source heat pump systems for sustainable houses. Appl Therm Eng 2015;81:279–87. https://doi.org/10.1016/j.applthermaleng.2015.02.039.
[16] Underwood C. On the design and response of domestic ground-source heat pumps in the UK. Energies (Basel) 2014;7:4532–53. https://doi.org/10.3390/en7074532.
[17] Christodoulides P, Aresti L, Florides G. Air-conditioning of a typical house in moderate climates with Ground Source Heat Pumps and cost comparison with Air Source Heat Pumps. Appl Therm Eng 2019;158. https://doi.org/10.1016/j.applthermaleng.2019.113772.
[18] European Committee for Standardization-CEN. EN 14825:2022, Air conditioners, liquid chilling packages and heat pumps, with electrically driven compressors, for space heating and cooling, commercial and process cooling-Testing and rating at part load conditions and calculation of seasonal performance 2022.
[19] OpenEnergyMonitor. HeatpumpMonitor.org 2025. https://heatpumpmonitor.org/ (accessed February 13, 2025).
[20] Kottek M, Grieser J, Beck C, Rudolf B, Rubel F. World map of the Köppen-Geiger climate classification updated. Meteorologische Zeitschrift 2006;15:259–63. https://doi.org/10.1127/0941-2948/2006/0130.